Available online at www.sciencedirect.com
SCIENCE DIRECT®
ELSEVIER
Environmental Modelling & Software 19 (2004) 177–183
Environmental Modelling & Software
www.elsevier.com/locate/envsoft

Comparison of wind erosion measurements in Germany with simulated soil losses by WEPS

R. Funk [a,*], E.L. Skidmore [b], L.J. Hagen [b]

[a] *Centre for Agricultural Landscape and Land Use Research, 15374 Müncheberg, Germany*
[b] *USDA, ARS, Wind Erosion Research Unit, Kansas State University, Manhattan, KS 66506, USA*

Received 20 September 2002; received in revised form 20 December 2002; accepted 18 February 2003

Abstract

The Wind Erosion Prediction System (WEPS) is a process-based model that simulates daily weather and field conditions along with hourly wind speeds and erosion. Its physical basis should allow model application to regions outside the US for which it was originally developed. The objective of this study was to compare results from measured wind erosion with simulated soil losses as a first example of WEPS use in Germany. Another objective was to introduce methods and techniques for quantifying wind erosion in preparation for model comparison studies to be undertaken within the Global Change and Terrestrial Ecosystems Soil Erosion Network. Comparisons between the measured and simulated erosion were based on single erosion events and outputs from the erosion submodel of WEPS. Multiple runs of the model were performed with varying roughness parameters to set the simulated threshold wind speed equal to that measured during the first erosion event after a tillage operation. This initial data set was used, depending on the rainfall or erosion, as the basis for the gradually changing roughness, crust cover and the fraction of erodible material on crust for all the following erosion events. Thus, the accuracy of the simulation depends much more on the relationship between erosion events, than on a good agreement for one single event. The results showed excellent agreement between measured and simulated erosion ($R^2 > 0.9$). This is mainly attributed to the good agreement with the four largest erosion events in which transport exceeded 100 kg/m width. Excluding these events, R^2 was reduced to about 0.6 for all other erosion events. Spatial and temporal variability of the soil transport were also reasonably simulated.

Keywords: Wind erosion; Wind Erosion Prediction System; Model validation

1. Introduction

Wind erosion is a serious problem in parts of northeastern Germany. These regions are characterized by sandy soils, low precipitation, and a transition to dry continental climatic conditions. The parent material was deposited in the last glacial period. The soils show a wide spectrum of characteristics concerning their substrates and hydrological features. In the immediate post glacial period large areas were covered with sandy aeolian deposits. Based on textural characteristics, today, about 30% of farmland in the region is susceptible to wind erosion (Frielinghaus and Schmidt, 1993).

The highest climatic erosivity, in March and April, coincide with the lowest soil resistance to wind erosion. The low resistance is caused by seedbed preparations and planting operations. The problem is further intensified by bare or very sparse residue cover on soil surfaces, as well as by the absence of shelterbelt leaves. Therefore, especially in spring, wind erosion occurs on fields of sugar beets, corn and other summer crops. The farmers generally work together on co-operative farms composed of large fields and use a high degree of mechanization. The main reasons for the increase in wind erosion risk in northeastern parts of Germany are caused by human activity resulting in (Frielinghaus, 1998):

– Increases in the field sizes and the removal of shelterbelts,
– Decreases in the ground water table and,
– Increases in the proportion of row crops like sugar beets and corn

* Corresponding author.

1364-8152/$ - see front matter © 2003 Elsevier Ltd. All rights reserved.
doi:10.1016/S1364-8152(03)00120-8

The dominant particle transport mode on the sandy soils is saltation. This damages plants by abrasion or burying, and fills ditches. It also impedes public transportation by reducing visibility and depositing material on roads. As an example of its severity, a soil mass discharge of about 1 ton/m width was measured in a single erosion event. Moreover, the critical field length to reach the saltation transport capacity was between 30 and 70 m (Schaefer et al., 1989; Funk, 1995). These results emphasize the importance of maintaining a permanent soil cover on the sandy soils in northeastern Germany.

Beginning with a German project to develop a wind erosion model, measurements of wind erosion have been carried out since 1991 (Kuntze and Beinhauer, 1989; Kruse, 1994). To facilitate model development, an erosion plot was installed and equipped with sediment traps and a meteorological station, to measure the wind erosion processes with high spatial and temporal resolution. Recently, a process-based Wind Erosion Prediction System (WEPS) model, under development in the US, became available for testing (Hagen et al., 1995). Hence, the objective of this study was to compare the results from wind erosion measurements with model-simulated soil losses as a first step in WEPS use in Germany. A second objective was to introduce methods and techniques for quantifying wind erosion in preparation for model comparison studies to be undertaken within the Global Change and Terrestrial Ecosystems Soil Erosion Network.

2. Materials and methods

2.1. Wind erosion measurements

Wind erosion was studied for 3 years on a 2.25 ha (150 m in square) experimental plot located about 50 km east of Berlin (52°39′ N, 14°11′ E). The average annual precipitation is 472 mm and the potential evapotranspiration is 590 mm. There is a climatic water deficit from March to September. The annual average wind speed is 4.4 m/s with the highest monthly average reaching 5.0 m/s in March. The landscape around the plot is flat and shelterbelts in the prevailing wind direction are about 800 m away. Crops grown on the field surrounding the plot during the 3 years of observation were carrots, corn and rye. The plot was maintained in the condition of a seedbed for the entire time. Four tillage operations in 1992 and five in 1993 were necessary to control weeds and to establish a fresh erodible surface after measured erosion events.

The soil is an Arenic Gleysol (FAO, 1998) with 88% sand, 6% silt and 6% clay in the topsoil (Table 1). Soil formation was influenced in the past by a ground water table at a depth of about 0.6 m. Wind erosion increased in the 1970s after the ground water table was lowered to more than 2 m.

Two methods were used to measure soil loss. The first used quantification of soil transport in the field, and the second used quantification of the deposits at the field boundary. These methods were compared three times during the course of the experiment.

Soil transport was measured with two sampler designs. Four SUSTRAs (SUspension Sediment TRAp, Fig. 1) were placed in the center of the field with inlet heights at 0.05, 0.15, 0.25 and 0.45 m above the soil surface. The SUSTRA was developed in a German Wind Erosion Research Project (Kuntze and Beinhauer, 1989) and has been used on several sites in Germany. The inlet flow velocity of the SUSTRA is adjustable by varying a slot on the backside of the vertical tube. The inlet flow rate is a compromise between achieving an isokinetic inlet flow and efficiently trapping the finest material. Based on the grain-size distribution of the experimental field, the SUSTRA was adjusted to provide maximum trapping efficiency for particles of the medium-to-fine sand fraction. Total efficiency was about 80% and, contrary to the name, the SUSTRA is more effective for collecting saltation-size than suspension-size particles. Weight of trapped sediment, along with wind speed and direction, were stored as 10-min averages in a data logger.

Meteorological data were recorded simultaneously to the measurements by the SUSTRA sediment traps with:

- wind speed at 10, 4, 1 and 0.5 m height
- air humidity
- air temperature at 3 and 1 m height
- soil temperature at 0.1 and 0.2 m depth
- soil surface moisture (by Infrared-reflection).

In addition to the SUSTRA samplers, 16 simple BOSTRA (BOttle Sediment TRAp, Fig. 2) samplers were arranged in a grid at 25 m intervals to measure the spatial distribution of the horizontal fluxes (Fig. 3).

The sediment trapped in the BOSTRA samplers was evaluated for each erosion event. These samplers are easily constructed and inexpensive, so they can be used in large numbers. The consistent form of the measured vertical sediment profiles allowed a reduction in the number of bottles from seven at the beginning of the measurement period to four per trap. The average efficiency of the BOSTRA is about 50% (Janssen, 1991; Sterk, 1993).

The theoretical assumption is that the total transport can be divided into saltation and suspension portions. This leads to the equation below, that describes the profile for the layer $0...z_{\mathrm{sal}}$ as saltation and all above the height z_{sal} as suspension.

$$Q = Q_{\mathrm{sal}} + Q_{\mathrm{sus}} = \int_0^{z_{sal}} q_{\mathrm{sal}}(z)\mathrm{d}z + \int_{z_{sal}}^{z_{up}} q_{\mathrm{sus}}(z)\mathrm{d}z \qquad (1)$$

Table 1
Soil properties in the upper 30 cm of the measuring field

(a) Fractions									(b) Contents				
>600 µm (%)	600–200 µm (%)	200–100 µm (%)	100–60 µm (%)	60–20 µm (%)	20–6 µm (%)	6–2 µm (%)	<2 µm (%)	Total carbon (mg/100 g)	Nitrogen (mg/100 g)	Phosphorus (mg/100 g)	Potassium (mg/100 g)	Magnesium (mg/100 g)	pH
3.7	27.3	41.2	15.1	3.2	2.3	1.5	5.7	950	93	12.5	2.1	3.7	7.1

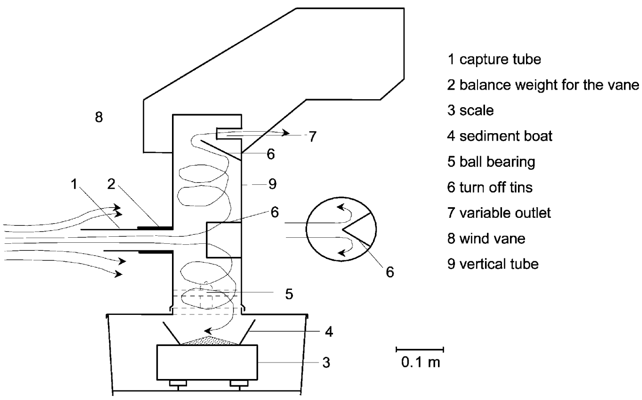

Fig. 1. Suspension Sediment Trap (SUSTRA), sketch of the design.

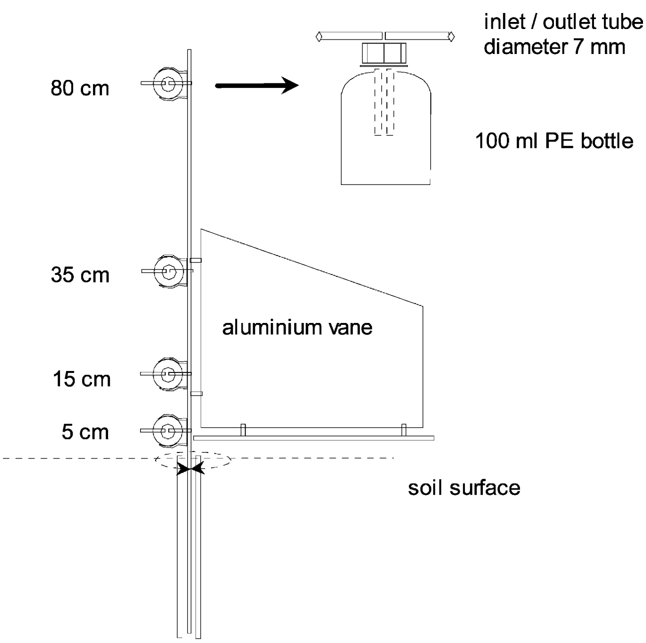

Fig. 2. Bottle Sediment Trap (BOSTRA).

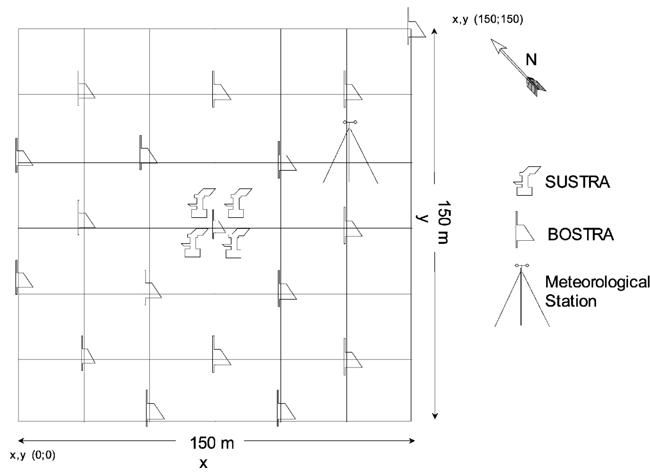

Fig. 3. Experimental plot with the positions of the used sediment traps.

In reality these modes of transport cannot be divided so sharply. In this study, saltation transport $q_{\mathrm{sal}}(z)$ was computed with an equation from Williams (1964)

$$q_{\mathrm{sal}}(z) = q_{\mathrm{sal}}(z_0)\mathrm{e}^{b_{\mathrm{sal}}z} \Leftrightarrow \ln(q_{\mathrm{sal}}(z)/q_{\mathrm{sal}}(z_0)) = b_{\mathrm{sal}}z \qquad (2)$$

where $q_{\mathrm{sal}}(z_0)$ is saltation transport immediately at the surface, b_{sal} is slope of the profile in a height versus ln $q_{\mathrm{sal}}(z)$ diagram, which is negative, and z is height above the soil surface.

Following Anderson et al. (1991), the vertical profile of suspension is calculated with

$$q_{\mathrm{sus}}(z) = q_{\mathrm{sus}}(z_1)\left(\frac{z}{z_1}\right)^{b_{\mathrm{sus}}} \Leftrightarrow \ln\frac{q_{\mathrm{sus}}(z)}{q_{\mathrm{sus}}(z_1)} = b_{\mathrm{sus}}\ln\frac{z}{z_1} \qquad (3)$$

where $q_{\mathrm{sus}}(z)$ is the suspension transport at the height z, b_{sus} is the slope of the suspension profile.

A significant problem in calculating the horizontal sediment flux profiles is estimating the border between transport modes, because they generally occur together in the first 1 m above ground. The measured profiles corresponded to the suspension profile very well, but the downward integration of the suspension equation results in an overestimation of the transport close to the surface. Therefore, the border between transport equations selected for use in the analysis is very important and influences the results substantially.

Based on wind tunnel tests, where the transport at the surface was measured, the transition height between suspension and saltation was set to 25 mm with $q_{sal} = q_{sus}$ at this height. Owen (1964) indicates the maximum height of saltation trajectories with less than $u_*^2/2g$, so that the assumed transition height is in this order of magnitude. Nevertheless, there is uncertainty about the calculated soil transport below 25 mm, because it amounted to about 60% of the total profile discharge. For that reason, all deposits at the field boundary and the measured soil transport of all erosion events from the corresponding wind direction were compared several times. There was a good agreement between both, and hence, the selected approach was confirmed (Funk, 1995). The horizontal flux for all traps was integrated up to a height of 1 m and for a 1 m width.

Fraction of total loss that was of suspension-size was estimated by setting the friction velocity (u_*) equal to the fall velocity (u_F) of single grains (Greeley and Iverson, 1987). All particles with fall velocities smaller than u_* were assumed to be suspension loss. Particle size was derived from the grain-size distribution curve of the surface soil. The friction velocity was derived from the wind profile, and the fall velocity was calculated using an approximation equation of Zanke (1982) for natural sediments, which is valid for all Reynolds numbers smaller than 2×10^5

$$u_F = \frac{11\nu}{d}\left(\sqrt{1 + 0.01D^{*3}} - 1\right) \quad (4)$$

where ν is the kinematic viscosity (m^2/s), ρ' is relative density, sediment and fluid $(\rho_S - \rho_F)/\rho_F$ (dimensionless), d is grain diameter (m), $D*$ is the sedimentological grain diameter $(\rho' g/\nu^2)^{1/3}d$.

Sediment from the BOSTRA samplers was evaluated in the same way and used to map the spatial distribution of sediment transport for each erosion event based on a surface mapping system. The total soil loss was estimated by summing up the transport rates of the leeward field boundaries.

2.2. Wind Erosion Prediction System (WEPS)

The Wind Erosion Prediction System (WEPS) is a process-based, daily time step model that simulates weather and field conditions (Hagen et al., 1995). Calculations for single events were made with the WEPS erosion submodel. If the surface conditions are susceptible and wind speed is above the threshold, erosion is computed on a subhourly basis (Hagen et al., 1995). There are several steps in the simulation procedure. First, the erosion submodel determines the static threshold friction velocity at which the erosion begins for each cell. The threshold is calculated based on surface conditions of: random and oriented roughness; flat biomass, crust, and rock cover; cover of loose, erodible aggregates on the crust; aggregate size distribution and density of uncrusted surface; and surface wetness. Soil loss and deposition are then calculated for subhourly periods, when friction velocity exceeds the static friction velocity threshold. To aid in the evaluation of off-site impacts, the soil loss is subdivided into components and reported as saltation/creep, total suspension, and fine particulate matter (PM-10) for each grid cell (Hagen et al., 1995; Hagen, 1997).

Constant input data included the dimensions of the simulated area, soil texture, and derived properties, such as aggregate size distribution and aggregate stability. Event-based inputs were soil surface conditions, such as roughness, crust cover, and measured 30-min average wind speeds, as well as the average wind direction for the day. Some weak events were analyzed together, if the duration was only a few hours per day and the days followed one another.

Unfortunately, not all necessary input parameters involving field surface conditions were measured, and therefore, some had to be estimated. The following protocol was used to estimate missing input parameters:

1. For the first erosion event after a tillage operation, the roughness parameters (random roughness and ridge height) were varied to set the simulated threshold wind speed equal to the measured threshold;
2. Inputs for the first erosion event after a tillage operation always got the highest roughness values and a non-crusted surface;
3. Erosion events after the first event always got inputs of decreasing roughness values (or at least the same), increasing crust cover fraction and a decreasing fraction of loose, erodible material depending on rainfall and erosion between the single events.

The surface crust cover fraction (SF_{cr}) was calculated based on cumulative rainfall in mm since the last tillage (CUMP) using an equation of Zobeck and Popham (1992, in WEPS: Technical description)

$$SF_{cr} = 0.36 + 0.0024\ \mathrm{CUMP} \quad (5)$$

The gradual change of surface conditions was continued until the next tillage operation. These assumptions appear reasonable to describe several erosion events in succession. The accuracy of the simulation depends much more on the relationships between events than on a good fit to one single event. Ridge width and ridge spacing were kept constant at 100 and 150 mm, respectively, because the influence of these parameters was not so critical.

Output from the stand-alone erosion model include the total loss on the field, the average loss per square meter and the mass crossing each field boundary. Total loss was subdivided into saltation/creep, suspension and PM10 proportions and obtained in a grid of 20 × 20 m as loss per square meter. The simulated soil loss per square meter was transformed into the discharge per meter width by accumulating it in transport direction and multiplying by the grid cell length of 7.5 m. Measured and simulated soil losses were compared at the centre point of the plot where both kinds of sediment traps were located.

3. Results and discussion

In all, 49 erosion events were measured during the 3 years of observation. Of these, 21 were selected and compared with simulated soil losses by WEPS. The dates, the measured and simulated soil transport (discharge) in the centre of the plot, as well as the input random roughness, ridge height, and crust fraction parameter are given in Table 2. In addition, the dates of the last tillage operation and the cumulative precipitation before the erosion event are listed. The results show excellent agreement between the measured and simulated soil losses with coefficient of determinations $R^2 = 0.98$ for the SUSTRA and $R^2 = 0.93$ for the BOSTRA (Figs. 4 and 5).

However, the apparent agreement between measured and simulated values must be discussed more fully, especially since the roughness parameters were estimated. The good agreements were mainly caused by the four largest erosion events (horizontal discharge > 100 kg/m). Three of them were also the first erosion events after tillage, so that they were most influenced by the subjectively fitted input data. Excluding these events, R^2 for all other (moderate to weak) events was reduced to 0.50 for the SUSTRA and 0.68 for the BOSTRA. Although not as strange, these are in reasonable agreement.

In the data fitting procedure, multiple runs were carried out with varying input parameters, and the set of parameters for the best fit between measured and simulated data was chosen. These parameters were then tested to determine if they were reasonable. However, such manipulations were only made for the first erosion event after a tillage operation. All inputs for the following erosion events were based on modifying these initial surface conditions in response to weather and erosion.

The best fits to the threshold wind speeds for first erosion events after tillage resulted in several possible sol-

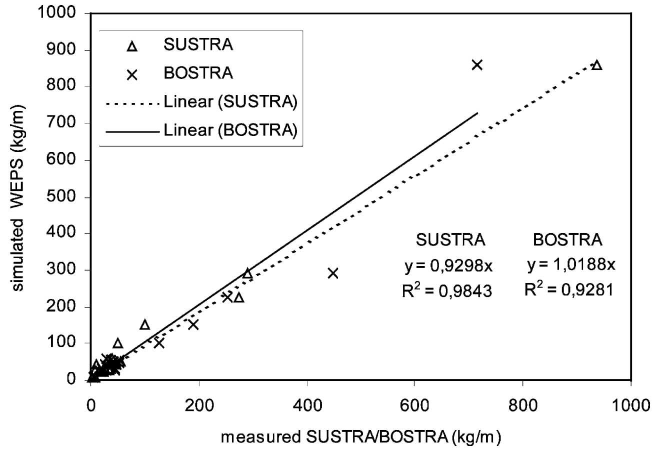

Fig. 4. Measured versus predicted soil transport for all selected wind erosion events in the center of the erosion plot.

Table 2
Measured and simulated transport rates and soil losses for selected erosion events and used roughness and crust parameters for calculation

Storm date	SUSTRA[a] (kg/m)	BOSTRA[a] (kg/m)	WEPS[a] (kg/m)	BOSTRA[b] (kg/m²)	WEPS[b] (kg/m²)	Random roughness	Ridge height (mm)	Crust fraction	Fraction of LEM	Last tillage operation	Cumulated prec. (mm)
14/04/92	33.8	44.7	27.9	0.52	0.37	4.0	20	0	1	08/04/92	4.8
21/04/92	936.4	714.9	860	10.52	10.46	3.0	0	0	1		7.4
04/05/92	7.3	8.8	6.8	0.17	0.15	3.0	0	0.42	0.4		25.3
12/05/92	7.5	23.9	29	0.38	0.37	4.0	10	0	1	05/05/92	11.6
15/05/92	1.85	7.3	8.7	0.12	0.11	3.0	0	0.42	1		27.3
18/05/92	54.6	43.3	50.5	0.40	0.59	3.0	0	0.42	1		27.5
27/05/92	31.5	52.6	42		0.53	3.0	0	0.42	1		27.5
05/06/92	101.2	190.2	151		1.8	3.0	0	0	1	03/06/92	0.1
10/06/92	27.9	52.5	45		0.5	3.0	0	0.37	1		5.6
29/07/92	274.1	254.5	225	3.61	2.4	2.0	0	0.42	1	11/06/92	27.3
08/04/93	7.77	6.5	7.8	0.26	0.11	4.0	25	0	1	29/03/93	20.3
20/04/93	50.3	126.2	101	1.82	1.29	4.0	10	0	1		4.5
23/04/93	22.6	18.2	24.4		0.3	3.0	5	0.37	1		4.5
26/04/93	39.9	29.6	57.3		0.64	3.0	5	0.4	0.6		4.5
30/04/93	36.4	45.6	30.9		0.4	2.5	5	0.4	0.6		4.5
10/05/93	46.6	48.6	44.6		0.64	2.0	0	0.4	0.2		5.3
12/05/93	25.5	22.4	32.5		0.35	2.0	0	0.4	0.2		5.3
02/06/93	15.5	22.9	28.4	0.49	0.33	3.0	15	0.4	1	26/05/93	18.6
16/06/93	11.7	25.8	43.6	0.22	0.68	3.0	10	0.6	1		60.8
08/07/93	289.1	449.1	292	3.75	3.53	4.0	0	0	1	22/06/93	0
27/07/93	31.3	37.6	56.2		0.78	3.0	0	0.43	0.2		28.4

[a] Transport crossing the field centre (kg per m width).
[b] Soil loss (kg/m²).

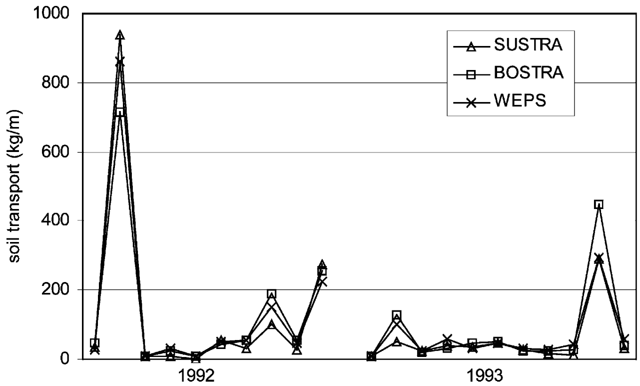

Fig. 5. Measured and predicted soil transport for all events in succession.

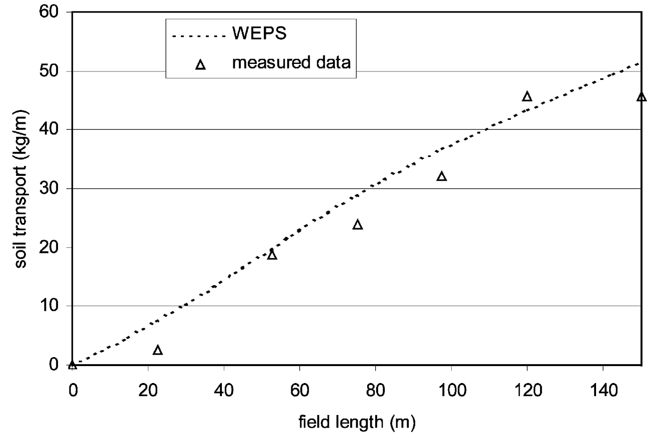

Fig. 6. Measured and simulated soil transport on the diagonal of the erosion plot ($R^2 = 0.92$), example of the erosion event at 12/05/92.

utions composed of combinations of random roughness (RR) and ridge height. To test the selected input data sets, measurements of RR by Helming (1992) were used. She measured RR values ranging from 4 to 10 mm for all common seedbed preparations in Germany. Multiple runs of the model were carried out and compared with the best fit within this range of RR. An example is given in Table 3, where all solutions for the event of 08/04/93 are summarized. This was the first event after a seedbed preparation. Solutions range between random roughness values of 4–10 mm with ridge heights of 25 mm and zero, respectively. The best fit was achieved for RR of 4 mm and a ridge height of 25 mm or RR = 10 mm and no ridges. All other solutions are between RR of 8 and 10 mm. A solution with higher RR and low or no ridge height seems to be most probable because differences in ridge heights of 25 mm are in the range of the cloddiness of a rough surface. Similar RR values between 6 and 13 mm were obtained by a visual comparison of our seedbed preparations with photos in the RWEQ handbook (Fryrear et al., 1998). Considering all this information, the selected roughness parameters seem acceptably close to the real possibilities.

The spatial variability of the measured and predicted soil transport was compared using the data of the BOSTRA samplers along the field diagonal (Fig. 6), and on

Table 3
Soil loss (kg/m²) in dependence of random roughness (RR) and ridge height (RH), erosion event at 08/04/93

RR	RH				
	0	10	15	20	25
0	4.18	2.81	2.27	0.53	0.12
2	4.14	2.77	2.24	0.52	0.12
4	2.43	1.24	1.09	0.48	0.11
6	0.72	0.44	0.39	0.36	0.1
8	0.37	0.18	0.15	0.13	0.1
10	0.11	0.05	0.04	0.03	0.03

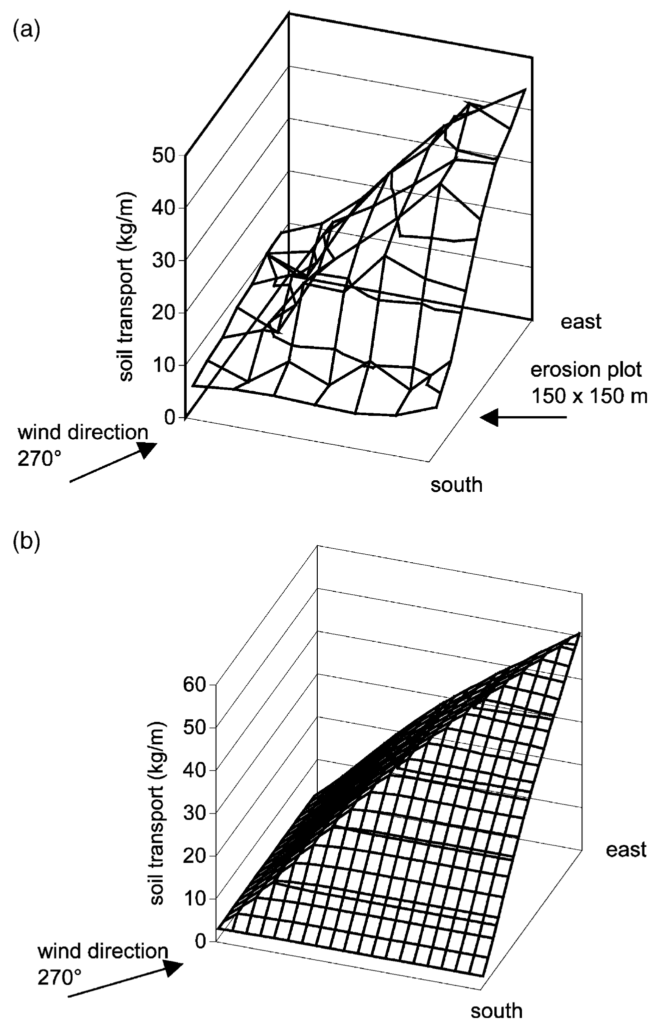

Fig. 7. Spatial variability of the measured (a) and simulated (b) soil transport on the erosion plot, example of the erosion event at 12/05/92; *x*, *y*-dimension=ground area of the erosion plot 150 × 150 m.

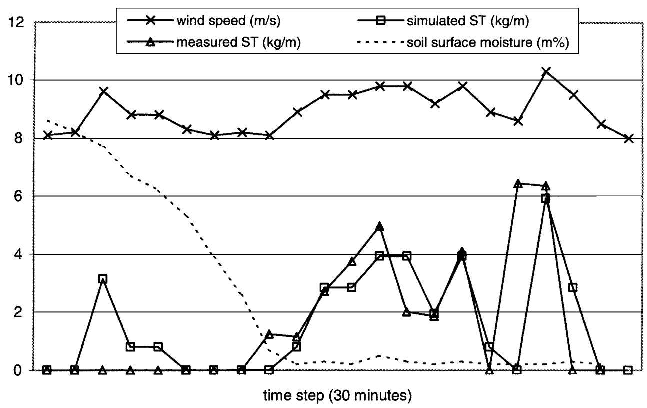

Fig. 8. Temporal variation in wind speed, surface moisture and soil transport of the erosion event at 08/04/93.

the entire plot (Fig. 7a). For comparison, the output matrix table of the erosion submodel is also illustrated (Fig. 7b). There is good agreement between simulated and measured for the increase of the total transport with the field length, with an R^2 of 0.92. It can be concluded that the basic transport principles, like the avalanching process at the beginning and the saturation of the saltation transport capacity after a short distance, are well described for this soil.

On average, the suspension component of soil discharge was 35% when estimated from the trapped sediment (<60 μm diameter), 26% when calculated from the friction velocity ($u_* = 0.54$ m/s), and 46% when estimated by the simulation model.

The temporal variations in soil transport within the erosion event on 20 April 1993 are shown in Fig. 8. Because soil surface moisture was not input into the model, the model calculated soil loss in the first 3 h before the actual event. Erosion in the field started after the decrease of soil surface moisture below 1% by mass. From that point, fluctuations in soil transport were correlated to wind speed fluctuations and well-simulated by WEPS.

4. Conclusions

Overall, the first comparison between measured and simulated soil losses by WEPS in Germany shows satisfying results. This includes the total soil loss for an event, the spatial variations on the field, and the temporal changes in transport capacity.

The estimation of all missing parameters was handled carefully with respect to all available information, in order to reduce the uncertainty and to minimize subjectivity. Further, varying the model inputs and studying the results has improved knowledge about essential parameters that need to be measured in the next field experiments. It would be useful for model comparison programs to have general information about how to easily calculate, derive or estimate missing input parameters. Some special cases, like changing surface moisture conditions or spatial variations in erodibility, will be evaluated in more detail in the next steps.

References

Anderson, R.S., Soerensen, M., Willets, B.B., 1991. A review of recent progress in our understanding of aeolian sediment transport. In: Aeolian Grain Transport 1, Mechanics. Acta Mechanica Supplementum 1. Springer-Verlag, Wien, New York.

FAO 1998. World Reference Base for Soil Resources. Food and Agriculture Organization of the United Nations, Rome.

Frielinghaus, M., Schmidt, R., 1993. Onsite and offsite damages by erosion in landscapes of east Germany. Farm land erosion. In: Wicherek, S. (Ed.), Template Plains Environment and Hills. Elsevier Science Publishers B.V, pp. 47–49.

Frielinghaus, M., 1998. Bodenschutzprobleme in Ostdeutschland. In: Richter, G. (Ed.), Bodenerosion, Analyse und Bilanz eines Umweltproblems: Wiss. Buchges., pp. 204–217.

Fryrear, D.W., Saleh, A., Bilbro, J.D., Schomberg, H.M., Stout, J.E., Zobeck, T.M., 1998. Revised Wind Erosion Equation. USDA, ARS, Technical Bulletin No. 1, June 1998.

Funk, R., 1995. Quantifizierung der Winderosion auf einem Sandstandort Brandenburgs unter besonderer Beruecksichtigung der Vegetationswirkung. ZALF-Report Nr. 16, Muencheberg, Germany.

Greeley, R., Iversen, J.D., 1987. Wind as a Geological Process on Earth, Mars, Venus and Titan. Cambridge Planetary Science Series 4. Cambridge University Press.

Hagen, L.J., Skidmore, E.L., Tatarko, J., Wagner, L.E., 1995. USDA Wind Erosion Prediction System: technical description. In: Proceedings of the WEPP/WEPS Symposium, Soil and Water Conserv. Soc, Des Moines, IA.

Hagen, L.J., 1997. Wind Erosion Prediction System: erosion submodel. Available from: http://www.weru.ksu.edu/symposium/proceed/hagen.pdf

Helming, K., 1992. Die Bedeutung des Mikroreliefs fuer die Regentropfenerosion. Ph.D. Thesis, Technical University of Berlin, 150 p.

Janssen, W., 1991. Prognostische Beschreibung eines Transportprofils bei Winderosion auf einem Ackerboden. Mitt. Dt. Bodenkundl. Ges. 65, 33–36.

Kruse, B., 1994. Wind erosion model development. Ecol. Model. 75/76, 289–298.

Kuntze, H., Beinhauer, R.T., Tetzlaff, G., 1989. Quantifizierung der Bodenerosion durch Wind. Mitt. Dt. Bodenkundl. Ges. 59/II, 1089–1094.

Owen, P.R., 1964. Saltation of uniform grains in air. J. Fluid Mech. 20, 225–242.

Schaefer, W., Neemann, W., Kuntze, H., 1989. Quantifizierung der Bodenerosion durch Wind—Feldmessungen. Mitt. Dt. Bodenkundl. Ges. 59/II, 1131–1134.

Sterk, G., 1993. Sahelian Wind Erosion research project. Report III. Description and calibration of sediment samples. Dept of ISWC, Wageningen Agricultural University, The Netherlands.

Williams, G., 1964. Some aspects of the aeolian saltation load. Sedimentology 3, 257–287.

Zanke, U., 1982. Grundlagen der Sedimentbewegung (Fundamentals of Sediment Movement). Springer Verlag, Berlin, Heidelberg, New York.

Zobeck, T.M., Popham, T.W., 1992. Influence of microrelief aggregate size and precipitation on soil crust properties. Trans. Amer. Soc. Agric. Eng. 35 (2), 487–492.